Ibn Al-Haitham Journal for Pure and Applied Sciences
Journal homepage: jih.uobaghdad.edu.iq
PISSN: 1609-4042, EISSN: 2521-3407
IHJPAS. 2026; 39(1)

# Synthesis and Characterization of Nanocomposites Derived from Grafted Carboxymethyl Cellulose

**Huda H. Saeed[1], Ruwaidah S. Saeed[2*], and El-Sayed Negim[3]**
[1,2]Department of Chemistry, College of Education for Pure Science (Ibn Al-Haitham), University of Baghdad, Baghdad, Iraq
[3]School of Materials Science and Green Technologies, Kazakh British Technical University, Kazakhstan
*Corresponding Author

Received: 31/May/2025
Accepted: 2/September/2025
Published: 20/ January /2026
doi.org/10.30526/39.1.4219



**Abstract**

Nanoparticle (NP)-based polymer nanocomposites have received significant attention in recent years, particularly those based on carboxymethyl cellulose (CMC). This study aims to synthesize and characterize of nanocomposites derived from grafted CMC. Because of the presence of polar functional groups, such as carboxyl and hydroxyl groups, in CMC, which contribute significantly to its strong adsorption capacity in metal structures, some research has indicated that this CMC is effective as a corrosion inhibitor, especially after being coated with NPs, as it protects metal surfaces from corrosion and helps them create a protective layer. In this study, nanocomposites derived from grafted CMC were synthesized. Initial CMC underwent a reaction with thionyl chloride in dimethylformamide (DMF) to produce CMC-Cl [I]. The CMC-Cl[I] reaction with various amines in DMF yields grafted CMC [II-X], which is subsequently blended with the natural biopolymer Chitosan to form blend polymers [XI-XIX]. Nanocomposites were synthesized through the interaction of blend polymers (grafted CMC/CS) with NPs such as magnesium oxide NPs (MgONPs), silver NPs (AgNPs), and gold NPs (AuNPs). The structures of the synthesized nanocomposites were characterized using FT-IR, $^{1}$H-NMR, FESEM, and TEM. An investigation into the corrosion inhibition of blended polymers and nanocomposites on mild steel in 0.1 M HCl was conducted using weight-loss analysis. The results show that nanocomposites have a higher inhibition rate than blended polymers. Grafted CMC/CS/AuNPs [XXXI] reached an inhibition rate of 97% against the corrosion of carbon steel.

**Keywords:** Grafted carboxymethyl cellulose, Corrosion inhibition, Magnesium oxide nanoparticles, Nanocomposites.

## 1. Introduction

Carboxymethyl cellulose (CMC) is a cellulose derivative known to be the most common and widely used[1]. This is because its polar functional groups, such as carboxyl and hydroxyl groups, make it more effective at adhering to metal surfaces. People often use CMC in the food and pharmaceutical industries, but some research has shown that this cellulose derivative can also prevent corrosion[2,3]. It is a type of cellulose produced by combining sodium monochloroacetate with alkali cellulose. It is a polymer with several intriguing properties[4]; chemically stable, readily soluble, and non-toxic. It is also a biodegradable, inexpensive, biocompatible polymer that can form films[5]. The pharmaceutical, food, and packaging sectors frequently use it due to its safety and non-toxicity. CMC dissolves in water and acts as a stabilizer, making food-binding agents thicker[6]. Because CMC is a white, odorless, tasteless, and environmentally friendly water-soluble solid, it is used widely across many fields, including washing, paints, adhesives, textiles, paper, ceramics, food, and pharmaceuticals[7]. Because CMC has a higher viscosity, it adheres

better and acts as a stabilizer. This property makes it worthwhile in the food business as a thickening ingredient in ice cream, in medical goods as a coating for medicine capsules, and in pharmaceuticals as a gelling agent. On the other hand, it is excellent for the environment and can be modified chemically easily[8-10]. It has many hydroxyl and carboxyl groups in its structure, which makes it useful in many ways[11]. When CMC is combined with other polymers, such as CS. Chitosan is a natural polysaccharide and the second most common organic compound in nature, behind cellulose[12]. Chitosan is a weak base that is insoluble in water[13]. This feature is probably due to the strong hydrogen bonds that form between the chitosan molecular chains. It can, however, dissolve in weakly acidic water with a pH below[14]. When this happens, the glucosamine units ($-NH_2$) transform into a form that can mix with water ($NH_3^+$). The solubility of chitosan depends on where it comes from, how big its molecules are, and how much deacetylation it has[15]. Chitosan is a versatile chemical used in many fields, including medicine, agriculture, food stability, biocatalysis, and environmental applications. Chitosan has amino and hydroxyl groups that help it stick to metal surfaces, which is vital for its job as a corrosion inhibitor[16]. Over the past few years, biopolymers have been used to produce nanocomposites rapidly. Nanoparticles (NPs) such as gold, silver, and magnesium oxide are highly effective at inhibiting corrosion because they have a large surface area and are highly reactive[17]. Previous studies have demonstrated that NPs can prevent rusting[18]. Researchers are still looking at how to combine nanomaterials (NMs) with biodegradable polymers[19]. CMC is safe for living things, breaks down quickly, and is simple to find. CMC is often used to reduce and stabilize metal NPs (MNPs) because it is environmentally friendly and can be easily transformed into various forms. Nanoparticles improve the mechanical, thermal, biological, and barrier properties of biopolymers, which makes them more useful[20]. This study aims to synthesis and characterization of nanocomposites derived from grafted CMC.

## 2. Materials and Methods

### 2.1. Materials

Chemicals were provided by BDH, SCR, and CDH, gold NPs (AuNPs), silver NPs (AgNPs), and magnesium oxide NPs (MgONPs) by US, Research Nanomaterials, Inc

### 2.2. Instrumentation

The FT-IR spectra were recorded on a Shimadzu FTIR-8400S over the range 400 $cm^{-1}$ to 4000 $cm^{-1}$. The $^1$HNMR spectra were obtained using an Ultra Shield 400 MHz spectrometer from Bruker, University of Tehran, Iran. TMS was used as an internal standard, with DMSO as the solvent. Field-emission scanning electron microscopy (FESEM) and transmission electron microscopy (TEM) were performed at the University of Tehran, Iran.

### 2.3. Methods of synthesis

#### 2.3.1. Synthesis of CMC-Cl [I][21]

About 0.01 mol of CMC was combined with $SOCl_2$ (0.01 mol) in 15 mL of MDF and refluxed for 8 hr. The excess thionyl chloride and MDF were removed under vacuum.

#### 2.3.2. Synthesis of grafted CMC [II-X][22]

CMC-Cl [I] has been synthesised through the reaction of 0.1 g of CMC with 0.1 g of various amines, specifically 3,3'-dimethyl-[1,1'-biphenyl]. -4,4'-diamine, 3,3'-dimethoxy-[1,1'-biphenyl] -4,4'-diamine, benzene-1,4-diamine, 4-nitroaniline,4,6-dichlorobenzo[d]Thiazol-2-amine, sulfamethizole, trimethoprim, tacrine, 4-aminoantipyrine are combined in 20 mL of dimethylformamide (DMF), the mixture is refluxed for 8 hr. The solution was deposited onto a Petri dish and allowed to evaporate at ambient temperature.

#### 2.3.3. Synthesis of polymer blends [XI-XIX][23]

Solvent casting was used to fabricate polymer mixes. The grafted CMC [II-X] was dissolved in water and stirred for 1 hr. at room temperature to prepare the grafted CMC solution. Additionally, 1 gram of chitosan was dissolved in 49 mL of a 2% aqueous acetic acid solution and stirred for 1 h. at room temperature to prepare the chitosan solution. Two polymer solutions,

grafted CMC [II-X] and chitosan, were blended in a 1:1 ratio to create a homogeneous solution using a hotplate stirrer for 1 hr following the amalgamation of the two polymer solutions.

### 2.3.4. Synthesis of grafted CMC/CS nanocomposites [XX-XXXI][24]

To help (magnesium, silver, or gold) NPs stick together in the composite matrix, 100 mg of dried grafted CMC/CS was added to 50 mL of MgONPs, AgNPs, or AuNPs solution at a concentration of 250 mg/L. For three hours, a hotplate stirrer was used to do this.

### 2.3.5. Corrosion inhibition[25]

The chemical composition of carbon steel samples is as follows: C, 0.20; Fe, 99.23; Cu, 0.18; Si, 0.27; Mn, 0.05; Ca, 0.02; and S, 0.05. The gravimetric method, especially weight loss, is perhaps the most widely used method for measuring inhibition. The weight-loss method is easy to use and provides reliable results, making it the standard for measuring in various corrosion-monitoring systems. This study used 250 mL beakers containing 100 mL of the testing solution at room temperature, with total immersion, to measure weight loss. Weigh the iron coupons and hang them in a beaker by a rod and hook. The coupons were exposed for 6 hr, cleaned with distilled water, dried, and then weighed again. The weight loss, measured in grams, is the difference between the weight of the iron coupons before and after they were placed in different testing solutions. Using the following law, the inhibition efficiency % was calculated.

I.E.= (Wu-Wi /Wu)×100

Wu stands for the weight loss in control solution, Wi represents the Loss in weight in the solution of inhibitor, I.E. stands for the Inhibition efficiency in inhibitor solution.

## 3. Results

The reaction of CMC with thionyl chloride in DMF made CMC-Cl [I]. The FTIR spectra of CMC-Cl showed a peak at 1732 $cm^{-1}$, which is believed to come from the carbonyl group of acyl chloride. A grafted CMC was made by mixing CMC-Cl with various amines in DMF. The FT-IR spectra of polymer [II] have a strong peak at 3367 $cm^{-1}$, showing that the OH stretching occurs because of hydrogen bonding. The little peaks at 2924 $cm^{-1}$ and 2874 $cm^{-1}$ are C-H stretch vibrations, and the band at 1654 $cm^{-1}$ comes from the amide group. The $^{1}$H-NMR spectrum of grafted CMC[II] shows a signal at δ 8.13 ppm that comes from the amide proton (C=O-NH). There are several peaks in the range of δ (6.97–7.96) ppm, which is where aromatic protons are found. A single signal at δ(2.59–2.90) ppm shows six protons from two $CH_3$ groups. The peak that shows $CH_2COOH$ on $C_6$ of CMC is around (3.83–3.96) ppm. The signals between 2.10 and 2.37 ppm are for ($H_2$, $H_3$, $H_4$, $H_5$) of CMC, whereas the signals between 4.64 and 4.81 ppm are for H1 of CMC. Signals show the OH group of CMC at 5.96 ppm, and signals demonstrate the $CH_2COOH$ group on $C_6$ of CMC at 12.6 ppm[26,27].

Grafted CMC, the FT-IR results indicated that the blended polymer made from CMC and CS had a high level of miscibility. The broadening of the bands in the (2400–3600) $cm^{-1}$ range indicates that there is strong hydrogen bonding between the amino groups of CS and hydroxyl groups of CMC. The peak at 1647 $cm^{-1}$ for the (C=ONH) functional group. Making grafted CMC/CS nanocomposites with MgONPs, AgNPs, and AuNPs. FT-IR data of nanocomposites [XX] show that the peaks at 3288 $cm^{-1}$ are due to O-H stretching caused by hydrogen bonds between and within molecules. The peaks at 2861 and 2920 $cm^{-1}$ are due to asymmetric and symmetric stretching vibrations of C-H from alkyl groups. The bonding of ( MgO, Ag, Au) NPs in the range of 400 to 800 $cm^{-1}$ also supports the idea that particles are forming[28,29].

### 3.1. FESEM assay[30]

The surface morphology differs for grafted CMC, as illustrated in **Figure 1**. **Figure 2** depicts grafted CMC blended with CS, while **Figure 3** presents grafted CMC/CS/MgONPs. **Figure 4** showcases grafted CMC/CS/AgNPs, and **Figure 5** features grafted CMC/CS/AuNPs. Following the addition of CS to the grafted CMC, the results indicate alterations in the composite membrane's surface topography, significantly affecting cell spreading. The FESEM image

indicates a homogeneous dispersion of NPs over the matrix surface. The average particle size of grafted CMC [VIII] ranges from 642 to 782 nm. The average particle size of the grafted CMC blend with CS [XVII] ranges from 141 to 166 nm, while the average particle size of the grafted CMC/CS/MgO ranges from 48 to 80 nm in the presence of Mg. The average particle size of grafted CMC/CS/Ag ranges from 49 to 58 nm in the presence of silver, whereas the average NP size for gold NP ranges from 28 to 43 nm. The NPs exhibit a homogeneous distribution across the matrix surface. The particles in the nanocomposite film exhibited an almost spherical shape. Nonetheless, specific clusters of NPs were also observed, and the surface showed a degree of roughness. A uniform distribution of AuNPs in CMC/CS and robust NP adhesion to the polymer were demonstrated. The grafted CMC/CS mixture, together with NPs, forms new hydrogen bonds by disrupting the tight intramolecular hydrogen-bond network in CMC, thereby creating an adsorption site between the inhibitor and the metal.

### 3.2.TEM assay[31-33]

The TEM picture shows the improved CMC/CS solution, which was drop-cast with AgNPs and AuNPs. The (Ag, Au) NPs are spread out equally and are shaped like half-spheres. The particles are close together and point in opposite directions. Now that we have improved the CMC/CS, the AuNPs and AgNPs are more stable. The TEM image shows that the grafted CMC/CS/AgNPs and AuNPs are between 50 and 100 nm in size, as illustrated in **Figures 6** and **7**. Particles were spherical and had a thin layer of silver and gold around the grafted CMC/CS. TEM micrographs showed that the grafted CMC/CS was surrounded by layers of silver and gold nanostructures of uniform size. Gold and silver particles appeared to cover the grafted CMC/CS, leading to the growth of the CMC/CS/AgNPs and CMC/CS/AuNPs, as shown in **Tables 1-3** and **Schemes 1-3**.

**Table 1.** The FT-IR of polymers [II-X]

| Com. No. | (O-H) of CMC | (C-H) aliph. | (C=O) amide | (C=C) | (C-O-C) |
|---|---|---|---|---|---|
| [II] | 3367 | 2924,2874 | 1654 | 1590 | 1017 |
| [III] | 3345 | 2928,2867 | 1660 | 1579 | 1037 |
| [IV] | 3409 | 2930,2856 | 1680 | 1572 | 1033 |
| [V] | 3268 | 2922,2854 | 1647 | 1591 | 1023 |
| [VI] | 3306 | 3009,2869 | 1657 | 1594 | 1013 |
| [VII] | 4513 | 2930,2883 | 1661 | 1578 | 1030 |
| [VIII] | 3363 | 2935,2889 | 1651 | 1600 | 1035 |
| [IX] | 3317 | 2928,2835 | 1650 | 1591 | 1046 |
| [X] | 3316 | 2921,2870 | 1680 | 1584 | 1017 |

**Table 2.** The FT-IR of blend polymers [XI-XIX]

| Com. No. | υ (O-H) and (N-H) | υ (C-H) aliph. | υ (C=O ) amide. | υ (C=C) c | υ (-$CH_2$-O-CO) | υ (C-O-C) |
|---|---|---|---|---|---|---|
| [XI] | 3303 | 2973,2885 | 1647 | 1600 | 1274 | 1046 |
| [XII] | 3377 | 2921,2854 | 1648 | 1588 | 1241 | 1046 |
| [XIII] | 3356 | 2937,2885 | 1651 | 1601 | 1251 | 1051 |
| [XIV] | 3356 | 2925,2862 | 1640 | 1594 | 1255 | 1040 |
| [XV] | 3352 | 2915,2874 | 1648 | 1572 | 1255 | 1045 |
| [XVI] | 3341 | 2911,2874 | 1632 | 1564 | 1269 | 1021 |
| [XVII] | 3212 | 2920,2875 | 1640 | 1590 | 1259 | 1057 |
| [XVIII] | 3354 | 2918,2872 | 1640 | 1594 | 1251 | 1057 |
| [XIX] | 3350 | 2920,2874 | 1655 | 1585 | 1267 | 1058 |

**Table 3.** Inhibition efficiency of blend polymer and nanocomposites in different concentrations of all polymers and nanocomposites at a temperature of room

| Beaker No. | Compound | Conce. (ppm) | $W_1$ | $W_2$ | Loss in weight | %Loss in weight | I.E (%) |
|---|---|---|---|---|---|---|---|
| 1 | Control [HCl] | - | 7.524 | 5.588 | 1.936 | 25.730 | - |
| 2 | HCl+ grafted CMC/CS [ XVII] | 100 | 7.293 | 7.012 | 0.281 | 3.853 | 85.485 |
| 3 | HCl+ grafted CMC/CS [XVII] | 200 | 7.754 | 7.495 | 0.259 | 3.340 | 86.621 |
| 4 | HCl+ grafted CMC/CS /MgONPs [XXIX] | 100 | 7.392 | 7.202 | 0.19 | 2.570 | 90.185 |
| 5 | HCl+ grafted CMC/CS /MgONPs [XXIX] | 200 | 7.761 | 7.590 | 0.171 | 2.203 | 91.167 |
| 6 | HCl+ grafted CMC/CS /AgNPs[XXX] | 100 | 7.495 | 7.384 | 0.111 | 1.480 | 94.266 |
| 7 | HCl+ grafted CMC/CS /AgNPs[XXX] | 200 | 7.593 | 7.489 | 0.104 | 1.369 | 94.628 |
| 8 | HCl+ grafted CMC/CS /AuNPs[XXXI] | 100 | 7.501 | 7.411 | 0.090 | 1.199 | 95.351 |
| 9 | HCl+ grafted CMC/CS /AuNPs[XXXI] | 200 | 7.453 | 7.414 | 0.039 | 0.523 | 97.985 |

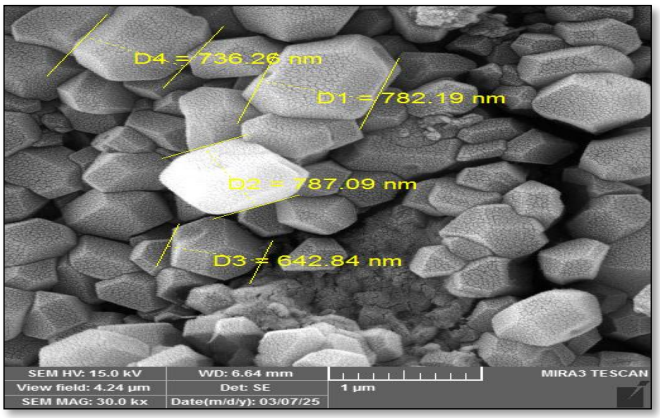


**Figure 1.** FESEM of grafted CMC[VIII]

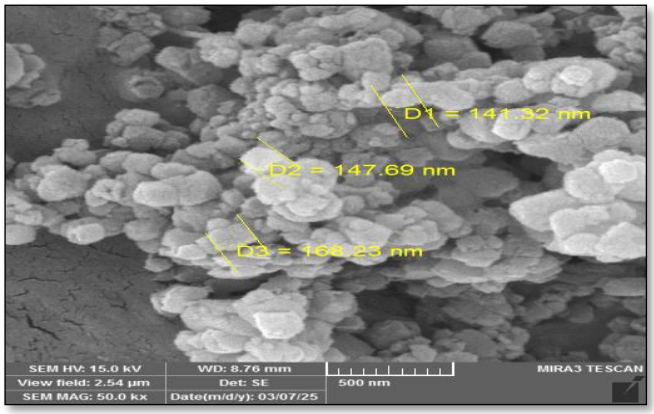


**Figure 2.** FESEM of grafted CMC/CS[XVII]

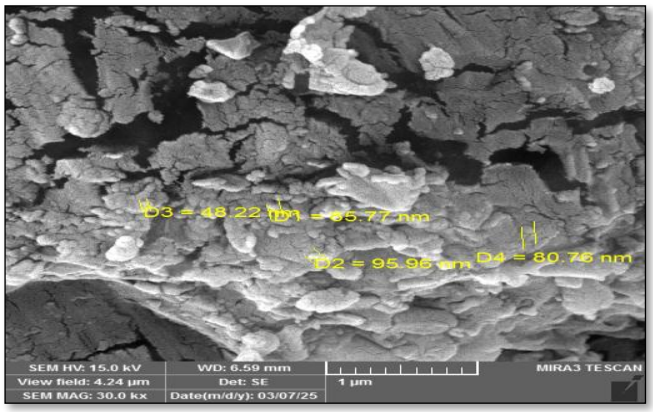


**Figure 3.** FESEM of grafted CMC/CS/MgONPs[XXIX]

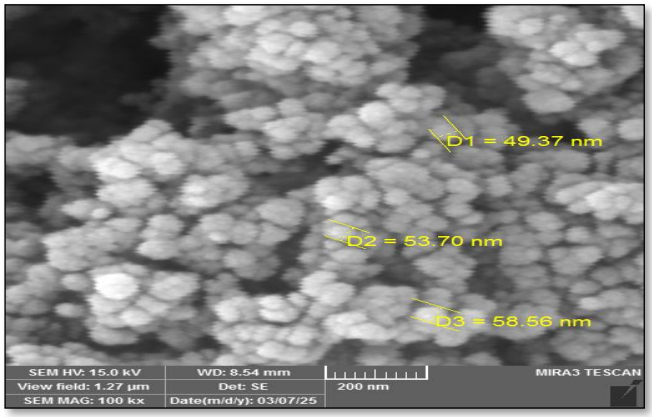


**Figure 4.** FESEM of grafted CMC/CS/AgNPs[XXX]

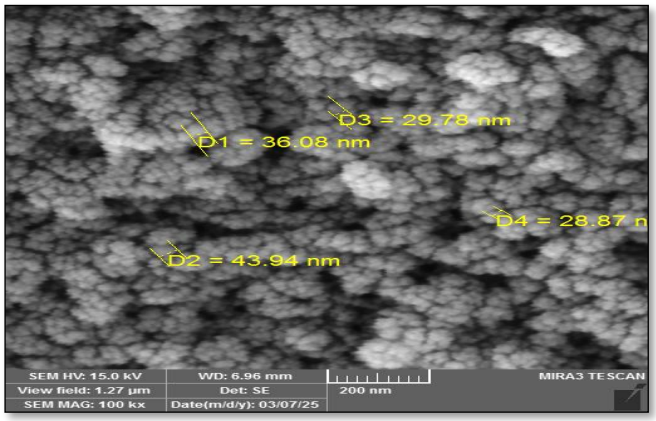


**Figure 5.** FESEM of grafted CMC/CS/AuNPs[XXXI]

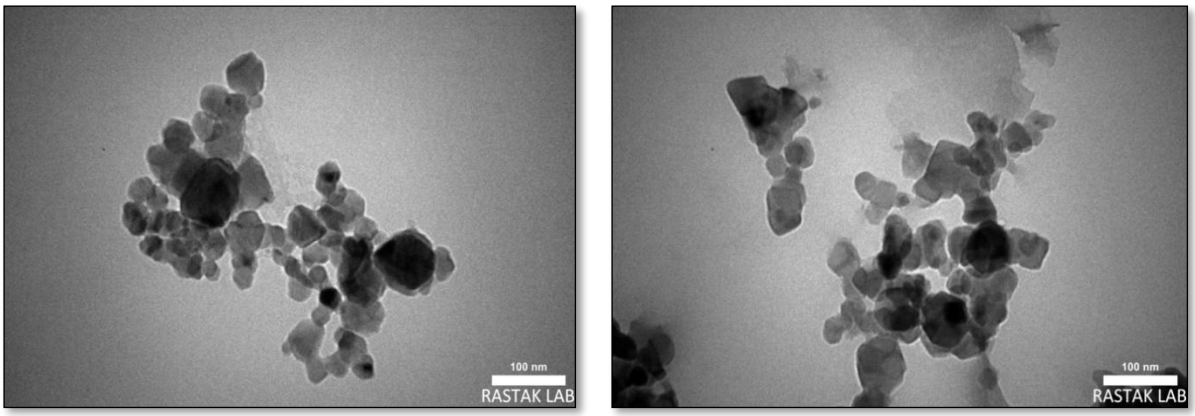


**Figure 6.** TEM of grafted CMC/CS/AgNPs

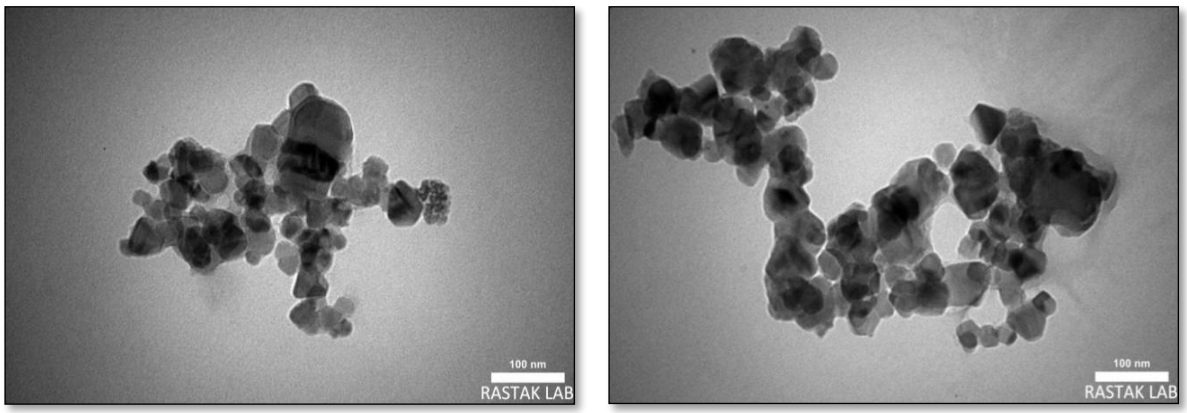


**Figure 7.** TEM of grafted CMC/CS/AuNPs

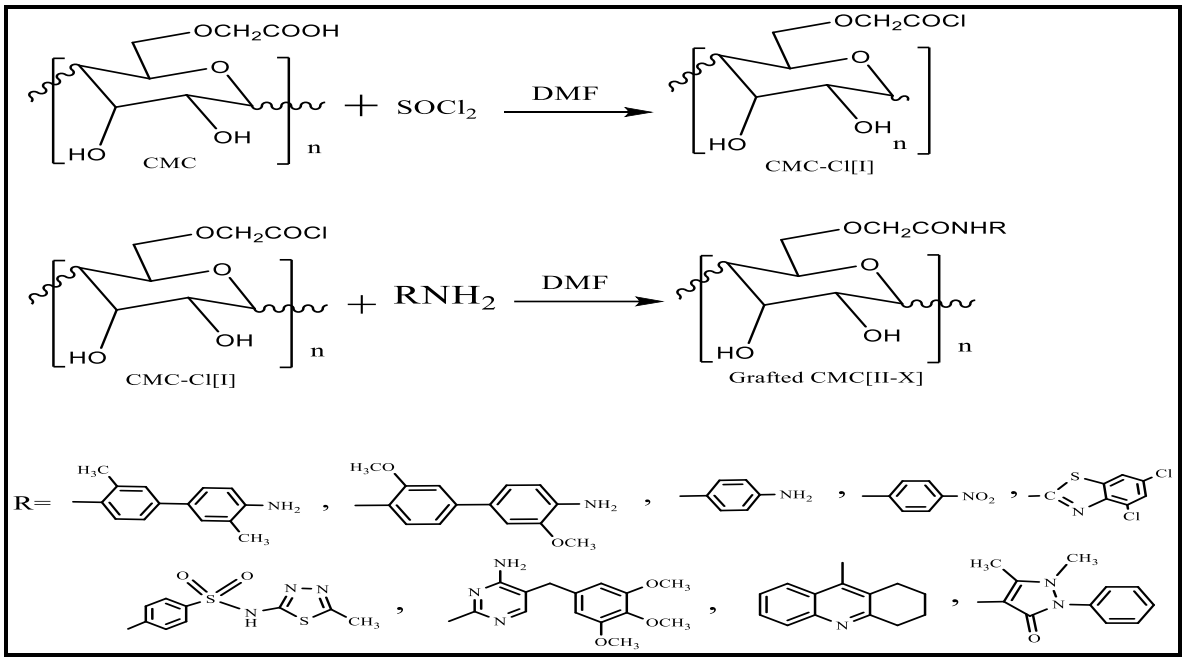


**Scheme 1.** Synthesis of grafted CMC[I-X].

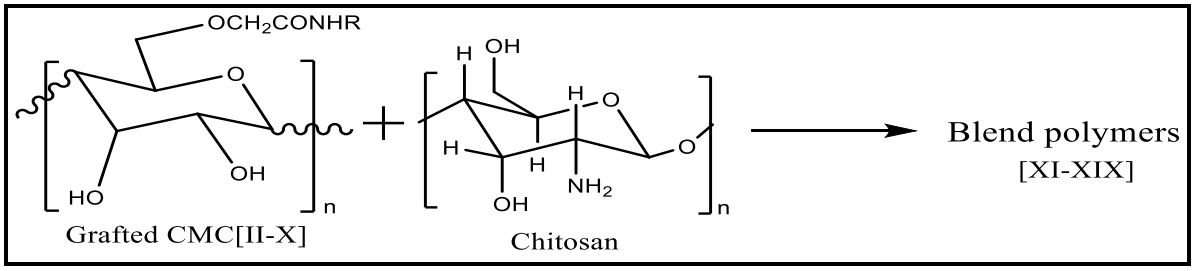


**Scheme 2.** Synthesis of blend polymers[XI-XIX].

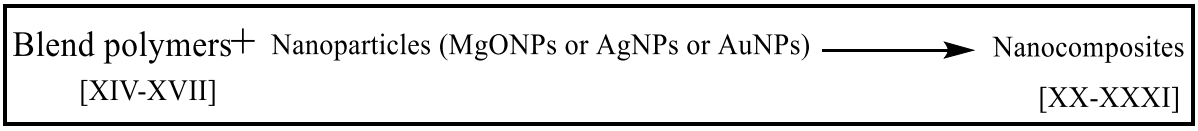


**Scheme 3.** Synthesis of nanocomposites [XX-XXXI].

## 4. Discussion

Nanocomposites and their blend polymers have been shown to make carbon steel far less prone to corrosion in acidic environments. The azomethine group, electronegative atoms (N, S), and p electrons in aromatic systems are all reasons why this happens[30].

The inhibitor compounds bind to the iron atoms via empty (d) orbitals, which are like spots that grab electrons. When the empty $^{3}$d orbitals of Fe coincide with the p-orbital electrons in the inhibitor, they form coordinated bonds. The methoxy groups on the aromatic ring exert an inductive effect, making the ring more active and increasing electron density.

These modifications can make it much easier for the inhibitor to absorb, which boosts both protection and adsorption. The study indicates that compounds that adhere to the metal surface act as adsorption inhibitors, preventing corrosion. It's also important to note that NPs, CMCs, and CS compounds can enhance protection by forming a thin, inactive surface layer on the material. This approach keeps harmful chemicals from reaching the metal[32,33].

This method either inhibits or slows redox processes in corrosion systems or renders dissolved oxygen ineffective. MgONPs, AgNPs, and AuNPs can protect metal surfaces against corrosion and form a protective layer. The results also showed that the nanocomposite grafted CMC/CS/AuNPs[XXXI] reached an inhibition rate of 97% against the corrosion of carbon steel[34].

## 5. Conclusion

The current study seeks to synthesize nanocomposites via reactions initiated by altering CMC-Cl with different amines. Certain synthesized compounds and polymers exhibited satisfactory FT-IR, $^{1}$H-NMR, FESEM, and TEM analyses that corresponded with data documented in the references. Finally, study the corrosion inhibition of blended polymers and nanocomposites in 0.1 M HCl on mild steel. The nanocomposites exhibit superior inhibitory efficiency compared to the blended polymer. The enhanced efficiency of the nanocomposites relative to the mixed polymer may be attributed to their NPs, resulting in the following efficiency hierarchy: [grafted CMC/CS/AuNPs [XXXI] > CMC/CS/AgNPs [XXX] > CMC/CS/MgONPs [XXIX] > CMC/CS [XVII]. The weight-loss data indicate that both surface coverage and inhibitory efficiency increase with increasing concentrations of the chemicals. The enhancement in inhibition efficiency with increasing inhibitor concentration may be attributed to the rise in –O–, –OH, and –COOH groups, which elevates the surface coverage of CMC molecules at higher concentrations.

## Acknowledgment

The authors thank the teaching staff of the Chemistry Department at the College of Education for Pure Sciences (Ibn Al-Haitham) and everyone who contributed to the completion of this research.

## Conflict of Interest

The authors have no conflict of interest.

## Funding

The research did not receive any financial funding from any institution.

## Ethical Clearance

Procedures were conducted in accordance with ethical standards, and guidelines of the institution, the National Research Council, and national laws were followed.

## References

1. Yassin AY, Abdelghany AM, Reda SS, Tarabiah AE. Structural, optical and antibacterial activity studies on cmc/pva blend filled with three different types of green synthesized zno nanoparticles. J Inorg Organomet Polym Mater 2023; 33:1855–1867. https://doi.org/10.1007/s10904-023-02622-y.
2. Hashem A, Farag S, Badawy SM. Carboxymethyl cellulose: Past innovations, present applications, and future horizons. Results Chem. 2025; 17, 102534. https://doi.org/10.1016/j.rechem.2025.102534
3. Zulkifli NASM, Ng K, Ang BC, Muhamad, F. Fabrication of water-stable soy protein isolate (SPI)/ carboxymethyl cellulose (CMC) scaffold sourced from oil palm empty fruit bunch (OPEFB) for bone tissue engineering. Ind Crops Prod. 2025; 224:120325. https://doi.org/10.1016/j.indcrop.2024.120325.
4. Liu Sh, Li H, Li X, Wang W, Rong Ch, Yang M, Wang Y, Wang J, Xu Y, Liang D, Xie Y. PVA-enhanced green synthesis of CMC-based lithium adsorption films. Carbohydr Polym. 2025; 349(PtA): 122973. https://doi.org/10.1016/j.carbpol.2024.122973.
5. El-naggar AM, Alsulaymani LA, Kamal AM, Albassam AA, Lakshminarayana G, Mohamed MB. Polyvinyl alcohol/carboxymethyl cellulose blended polymers doped with PPy/milled MWCNTs filler for flexible optoelectronic and energy storage applications. Polym Test. 2024; 138(5):108551. https://doi.org/10.1016/j.polymertesting.2024.108551.
6. Taha AG, Radwan MF, Abdu ME, Ali NM, Eletmany MR. Green synthesis and applications of modified schiff base chitosan derivative. Afr J Biomed Res. 2024; 27(4s):58–64. https://doi.org/10.53555/AJBR.v27i4S.3498.
7. Li L, Baig MI, de Vos WM, Lindhoud S. Preparation of sodium carboxymethyl cellulose–chitosan complex membranes through sustainable aqueous phase separation. ACS Appl Polym Mater. 2023; 5(3): 1810–1818. https://doi.org/10.1021/acsapm.2c01901
8. Albanda WH, Saeed MH, Abdullah MZ. Enhancing structural and optical properties of PVA: CMC

blend by NiO nanoparticle. J Nanostruct. 2025; 15(2):459-466. https://doi.org/10.22052/JNS.2025.02.007.
9. Abdelghany AM, Elamin NY, Younis SH, Ayaad DM. Polyvinyl pyrrolidone/ carboxymethyl cellulose (PVP/CMC) polymer composites containing CuO nanoparticles synthesized via laser ablation in liquids. J Mol Liq. 2024; 403(1):124857. https://doi.org/10.1016/j.molliq.2024.124857.
10. Akhlaq M, Maqsood H, Uroos M, Iqbal I. A Comparative study of different methods for cellulose extraction from lignocellulosic wastes and conversion into carboxymethyl cellulose. Chemistry Select. 2022; 7(29):1-9. https://doi.org/10.1002/slct.202201533.
11. Khoramabadi HN, Arefian M, Hojjati M, Tajzad I, Mokhtarzade A, Mazhar M, Jamavari A. A review of polyvinyl alcohol/ carboxymethyl cellulose (PVA/CMC) composites for various applications. J Compos Compd. 2020; 2(3):69-76. https://doi.org/10.29252/jcc.2.2.2.
12. Mahmoud DE, Billa N. Physicochemical modifications in microwave-irradiated chitosan: Biopharmaceutical and medical applications. J Biomater Sci Polym Ed. 2024; 35(6):898-915. https://doi.org/10.1080/09205063.2024.2306695.
13. Kruczkowska W, Kłosiński KK, Grabowska KH, Gałęziewska J, Gromek P, Kciuk M, Kałuzińska-Kołat Ż, Kołat D, Wach RA. Medical applications and cellular mechanisms of action of carboxymethyl chitosan hydrogels. Molecules. 2024; 29(18):4360. https://doi.org/10.3390/molecules29184360.
14. Khadatare V, Parab M, Kondekar S, Patil S, Natu D, Solanke S. Chitosan as a sustainable biopolymer: A comprehensive review. J Pharmacogn Phytochem. 2025; 14(2):102-107. https://www.doi.org/10.22271/phyto.2025.v14.i2b.15280.
15. Hamdi M, Sun H, Pan L, Wang D, Sun M, Zeng Z, Li S, Dong Q, Su F. Chitosan and its derivatives as potential biomaterials for biomedical and pharmaceutical applications: A comprehensive review on green extraction approaches, recent progresses, and perspectives. Eur Polym J. 2025; 229(8):113882. https://doi.org/10.30526/38.1.3501.
16. Olayemi J, Olayemi S, Adeyemi O, Lawal O, Adams F, Tijani A. Effect of organic solvents on the synthesis and characterization of carboxymethyl cellulose from sawdust. ASRJETS. 2020; 69(1):195-215. https://asrjetsjournal.org/American_Scientific_Journal/article/view/5642.
17. Yan Q, Wei P, Peng R, Tian Sh, Li D, Tong Y, Ni J, Liu L, Xiong B. Controllable synthesis of carboxymethyl cellulose and its application in tobacco sheets. Wuhan Univ J Nat Sci. 2023; 28(4): 341-350. https://doi.org/10.1051/wujns/2023284341.
18. Karimi M, Naimi-Jamal MR. Carboxymethyl cellulose as a green and biodegradable catalyst for the solvent-free synthesis of benzimidazoloquinazolinone derivatives. J Saudi Chem Soc. 2019; 23(2): 182-187. https://doi.org/10.1016/j.jscs.2018.06.007.
19. Salem SS, Hashem AH, Sallam AM, Doghish AS, Al-Askar AA, Arishi AA, Shehabeldine AM. Synthesis of silver nanocomposite based on carboxymethyl cellulose: antibacterial, antifungal and anticancer activities. Polym. 2022; 14(16):3352. https://doi.org/10.3390/polym14163352.
20. Alheety KA, Jamel NM, Abd Al-Hameed WM, Al-Rawi MS, Tomma JH. Synthesis and study of the biological activity of new compounds derived from 4-(5-phenyl-1,3,4-oxadiazole-2-yl)aniline. Russ J Org Chem. 2024; 60(7):1342-1347. http://dx.doi.org/10.1134/S1070428024070261.
21. Pettignano A, Charlot A, Fleury E. Carboxyl-functionalized derivatives of carboxymethyl cellulose: towards advanced biomedical applications. Polym Rev. 2019; 59(3):510-560. https://doi.org/10.1080/15583724.2019.1579226.
22. Pettignano A, Charlot A, Fleury E. Solvent-free synthesis of amidated carboxymethyl cellulose derivatives: Effect on the thermal properties. Polym. 2019; 11(7):1227. https://doi.org/10.3390/polym11071227.
23. Thomas S, Solomanb PA, Rejini VO. Preparation of chitosan-CMC blends and studies on thermal properties. Proc Technol. 2016; 24:721–726. https://doi.org/10.1016/j.protcy.2016.05.201.
24. Shlaka WA, Saeed RS. Gold and silver nanoparticles with modified chitosan /pva : synthesis, study the toxicity and anticancer activity. Nanomed Res J. 2023; 8(3):231-245. https://doi.org/10.22034/nmrj.2023.03.002.
25. Wang Y, Gao X, Qiu J, He W, Ma H. Enhanced anti-corrosion performance of sodium carboxymethyl cellulose coating on 5052 aluminium alloy via rapid gelation by metal ions. Colloids Surf. A, Colloids Surf. A Physicochem. Eng Asp. 2025; 709(9):136145. https://doi.org/10.1016/j.colsurfa.2025.136145.
26. Jimaa RB, Majid IY, Abdulrazzak FH, Hussein FH. synthesis and characterization of nano-multilayer

graphene grown by ambient pressure of chemical vapor deposition from naphthalene/ methanol. J Nanostruct. 2023; 13(3):830–836. https://doi.org/10.22052/JNS.2023.03.023.

27. Çelikçi N, Ziba CA, Dolaz M. Synthesis and characterization of carboxymethyl cellulose (cmc) from different waste sources containing cellulose and investigation of its use in the construction industry cellul. Chem Technol. 2022; 56(1-2):55-68. http://dx.doi.org/10.35812/CelluloseChemTechnol.2022.56.05.
28. Radmehr M, Marjani AP, Akhavan A. Synthesis and characterization of antibacterial CMC/AAc/ZnO nanocomposite superabsorbent using gamma radiation. Sci Rep. 2025; 15(1):9345. https://doi.org/10.1038/s41598-025-93884-8.
29. Yassen TM, AL-Azzawi AM. Synthesis and characterizationof newbis-schiff bases linked to various imide cycles. Iraqi J Sci. 2023; 64(3):1062-1070. https://doi.org/10.24996/ijs.2023.64.3.3.
30. Abdulsada ZS, Hassan SS, Awad SA. Removal of some heavy metals from polluted water using new schiff base for polyacrylamide with zeolite nanocomposites. Baghdad Sci J. 2024; 21(9):2838-2852. https://doi.org/10.21123/bsj.2024.8591.
31. Supriadi D, Ziska R, Awaludin A. Effect of isopropanol and ethanol on synthesis carboxymethyl cellulose (CMC) from coconut husk. IOSR J Pharm Biol Sci. 2021; 16(5Ser.I):24-30. https://doi.org/10.9790/3008-1605012430.
32. Gunathilake TMS, Ching YC, Chuah CH, Abd Rahman N, Nai-Shang L. pH-responsive poly(lactic acid)/sodium carboxymethyl cellulose film for enhanced delivery of curcumin in vitro. J Drug Deliv Sci Tech. 2020; 58(3):101787. https://doi.org/10.1016/j.jddst.2020.101787.
33. Odusote JK, Asafa TB, Oseni JG, Adeleke AA, Adediran AA, Yahya RA, Abdul JM, Adedayo SA. Inhibition efficiency of gold nanoparticles on corrosion of mild steel, stainless steel and aluminium in 1M HCl solution. Mater Today. 2021; 38(2):578-583. https://doi.org/10.1016/j.matpr.2020.02.984.
34. Savizi MR, Abbasi R. Effect of carboxymethyl cellulose on the corrosion behavior of aluminum in H2SO4 solution and synergistic effect of potassium iodide. J Adhes Sci Technol. 2020; 34(1):1-15. https://doi.org/10.1080/01694243.2020.1717803.